Personal and Ubiquitous Computing (2018) 22:511–524
https://doi.org/10.1007/s00779-018-1152-3

ORIGINAL ARTICLE

Wearing-independent hand gesture recognition method based on EMG armband

Yingwei Zhang[1,3,4,5] · Yiqiang Chen[1,3,4,5] · Hanchao Yu[2,3,5,7] · Xiaodong Yang[1,3,4,5] · Wang Lu[1,3,4,5] · Hong Liu[6,7]

Received: 9 August 2017 / Accepted: 30 October 2017 / Published online: 11 May 2018

Abstract
Electromyographic (EMG) armband with electrodes mounted around the user's forearm is one of the most ergonomic wearable EMG devices and is used to recognize fine hand gesture with great popularity. Definitely, the distributions of signal differ greatly in different wearing positions of armband based on the physiological characters of EMG, which will cause the performance decline and even the inapplicability of the recognition model built in one position. Hence, this paper proposes a wearing-independent hand gesture recognition method based on EMG armband. To eliminate the influence of wearing position, Standard Space is proposed in this paper. Based on the sequential features of EMG in different scales, the wearing position of armband is predicted and helps unify the original features to the proposed space. Then, with the unified signals, fine hand gesture can be recognized accurately and robustly with lightweight Random Forest (RF). The experimental results showed that the recognition accuracy of the proposed method was 91.47% approximately. And compared with the method without fine feature extraction and feature space unification, the performance was improved by 10.12%.

Keywords Human-computer interaction · Hand gesture recognition · Electromyographic (EMG)

1 Introduction

With the continuous development of bioelectricity signal sensing technology, the electromyographic -based hand gesture recognition technology is used more and more widely [1], which has been a main hand gesture recognition solution besides methods based on computer vision [2], inertial measurement unit [3], ultrasound [4], electromagnetic wave [5], ultrasound imaging [6], and so on. Compared with other hand gesture recognition solutions, EMG-based techniques provide us withsignificant opportunity to realize natural human-computer interaction (HCI) by directly sensing and decoding human muscular activity [7, 8]. These methods are capable of distinguishing subtle finger configurations, hand shapes, and wrist movements. What's more, EMG is insensitive to environmental light and sound noise, providing a robust HCI way. Non-intrusion and quick-response are also the advantages of this method. Recently, the EMG-based technique

✉ Yiqiang Chen
yqchen@ict.ac.cn

Yingwei Zhang
zhangyingwei@ict.ac.cn

Hanchao Yu
yuhanchao@ict.ac.cn

Xiaodong Yang
yangxiaodong@ict.ac.cn

Wang Lu
luwang@ict.ac.cn

Hong Liu
hongliu@sdnu.edu.cn

1 Institute of Computing Technology, Chinese Academy of Sciences, Beijing, China

2 Chinese Academy of Sciences, Beijing, China

3 Beijing Key Laboratory of Mobile Computing and Pervasive Device, Beijing, China

4 University of Chinese Academy of Sciences, Beijing, China

5 Beijing Key Laboratory for Parkinson's Disease, Beijing, China

6 School of Information Science and Engineering, Shandong Normal University, Jinan, China

7 Shandong Provincial Key Laboratory for Distributed Computer Software Novel Technology, Jinan, China

has attracted more and more attentions of researchers. There are not only many hand gesture recognition methods proposed [9, 10], but also appearing many hand gesture recognition productions, such as Myo [11], gForce [12], DTing [13], and eCon [14].

The EMG used in hand gesture recognition is a kind of bioelectricity which is produced when skeletal muscle contracts. This signal can be used to determine which muscles are active and even the amount of force they produce. The active regions of the forearm differ greatly when performing different gestures. Hence, the motion can be identified according to EMG. EMG can be sensed by EMG sensor worn on upper forearm, which can reflect the movement intention of user's muscle while performing hand gestures [15].

Usually, there are two types of conventional EMG sensors. One is configured with electrodes that are precisely attached to muscle [16, 17] and another one uses array-like arrangement of electrodes to capture the activity under a certain area of the upper forearm [18, 19]. But both are not suitable solution for wearable device that need to be taken on and off quickly. EMG armband mounted on upper forearm which contains some electrodes is an emerging EMG sensing device, and it can not only satisfies the convenience requirement of body-worn device, but also records the subtle electrical activity produced by muscles on the surface of skin. There is a major challenge of this novel equipment, which is EMG armband's wearing style influences the performance of recognition. EMG signal's closely position dependence [21] property requires that the wearing position of EMG armband keep consistent during the process of using. Subtle wearing position change will cause the decline of recognition accuracy. The requirement that wearing position must keep invariant not only degrades the user experience, but also cannot be satisfied when the wearing position shift with the influence of outside force.

To solve the challenge aforementioned, this paper proposes a wearing-independent hand gesture recognition method based on EMG armband. Specifically, Standard Space is proposed in this paper to eliminate the influence of wearing position. Based on the sequential features of EMG in different scales, the wearing position of armband is predicted and helps unify the original features to the proposed space. Then, with the unified signals, fine hand gesture can be recognized accurately and robustly with lightweight RF. In addition, empirical mode decomposition (EMD) is applied to extract features in different scales at the preprocess period.

This paper is organized as follows: Section 2 reviews some related work; the description of the proposed approach will be detailed in Section 3; Section 4 will show the experimental process and performance evaluation; concluding remarks are given in Section 5.

2 Related work

Recently, with the development of biological electricity signal sensing technology [22] and due to the advantages showed by EMG-based hand gesture recognition technology, such as ability to recognize fine gestures, insensitiveness to environmental light and sound noise, non-intrusion, and so on, there have been numerous works on using EMG for HCI [23], in particular for recognizing hand and finger movement for gesture input and control. HCI puts forward high requirements for the wearing convenience of EMG devices. Therefore, we restrict our reviews mainly on the related work that uses body-worn ergonomic EMG equipments.

Some researchers explored fusion method that used EMG and other kinds of signal to realize high-accuracy hand gesture recognition. Zhang et al. [7] proposed a hand gesture recognition framework based on the fusion information of multi-channel EMG signals and three-axis accelerometers. In their work, the beginning and ending points of hand gesture segment were detected by the magnitude of EMG signal, and the sign language was recognized by Hidden Markov Model and Decision Tree. But EMG sensors used were required to locate over five fixed sites on the surface of forearm. Lu et al. [28] proposed an algorithmic framework used to process acceleration and surface EMG signals for gesture recognition. It included a novel segmentation scheme, a score-based sensor fusion scheme, and two new features. A Bayes linear classifier and an improved dynamic time-warping algorithm were utilized in the framework. In addition, a prototype system, including a wearable gesture sensing device, which embedded with a three-axis accelerometer and four surface EMG sensors, and an application program with the proposed algorithmic framework for a mobile phone, was developed to realize gesture-based real-time interaction. Jess MeIntosh et al. [9] acquired four channel EMG signals and four channel force sensitive resistor signals by wearable equipment placed on the wrist. Then, they realized a high-accuracy hand gesture recognition system EMPress.

Compared with fusion method, single-mode solutions that use EMG signal just is more convenient. Takamitsu Matsubara et al. [24] used a bilinear model to construct a multiuser myoelectric interface, where the original EMG was decomposed into motion-dependent part and user-dependent part. But as the paper mentioned, the user-dependent factors were not precise enough and placement problem of electrode was still open. Scott Saponas et al. [25] researched the real-time hand gesture recognition method based on EMG, and the experimental results demonstrate that the proposed real-time method obtained the recognition accuracy of 79, 85, and 88% respectively on three gestures, including pinching, holding a travel mug, and carrying a weighted bag. They further showed the generalizability of

this method across different arm postures and explored the tradeoffs of providing real-time visual feedback. Though the unobtrusive wireless forearm band was used, the wearing position was not taken into consideration in their work. David [26] designed a PC mouse commanded by EMG signals obtained from two muscles of the forearm, palmar longus and extensor digitorum. The experimental result showed that the classification accuracy was 87% on the predefined hand movements set: rest, flexion, extension, and closure. Khushaba [27] proposed a framework for multiuser Myoelectric interfaces by using canonical correlation analysis, where different users' signal was projected onto a unified-style space. The proposed method was able to overcome individual differences with accuracies of 83% across multiple users.

Though the methods described above get good recognition result, none of them takes the wearing position into consideration. Thus, the solutions aforementioned are far from realizing natural and harmonious hand gesture recognition system. Amma et al. [20] analyzed the effect of the scale of used electrodes and found that cross-session recognition typically suffered from electrode position change from session to session. So they presented two methods to estimate the electrode shift between sessions based on a small amount of calibration data. But the proposed method was based on an electrode array with 192 electrodes and only the condition of position shift was explored in this work. Myo armband produced by Canadian Thalmic company realized the goal of recognizing palm and arm status by eight channel EMG signals and nine inertial sensing unit signals. Though Myo was ring and the user could wear the device at any angles, user had to calibrate the equipment before using and this operation was not convenient.

All the aforementioned approaches tried to realize EMG-based high-accuracy interaction. However, most of them neglected the wearing position influence of EMG device. Though Amma C et al. taken the position shift into consideration, their work was based on an electrode array with 192 electrodes. How to realize wearing-independent and position shift robust hand gesture recognition is still an open research question.

3 Wearing-independent recognition method

The objective of this paper is to realize wearing-independent hand gesture recognition based on EMG acquired by body-worn armband, as showed in Fig. 1. Wearing-independent gesture recognition system consists of four parts, including inputting of gestures, valid feature extraction, wearing-independent gesture recognition, and the outputting of ultimate result. In the first part, original signal is acquired by EMG armband and the obtained signal will be filtered and segmented by preprocessing. In the next part, the segment of EMG will be decomposed into a serial of intrinsic mode functions (IMFs) by EMD, which can transform original signal to fine-grained components. Then, the features in time domain and frequency domain will be extracted from both original EMG and the IMFs. In the part of wearing-independent gesture recognition, we predict the wearing position of armband using features in current moment and previous T moments firstly. Following this, we unify the features to the proposed Standard Space according to wearing position. With the unified signals, fine hand gesture can be recognized accurately and robustly by RF algorithm. In the last part, the recognition result will be outputted.

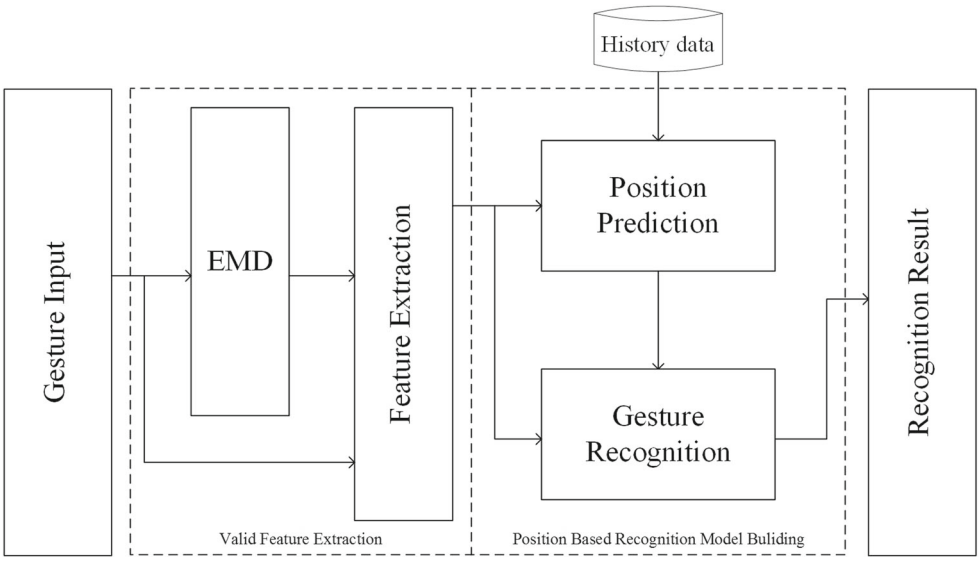

Fig. 1 Wearing-independent hand gesture recognition method based on EMG armband

The details of the proposed wearing-independent gesture recognition method will be given latter.

3.1 Fine-grained feature extraction method based on EMD

EMG is a kind of biological electricity signal, which has the non-linear and non-stationary properties. Traditional signal analysis method is based on the hypothesis that signal is composed of predefined basis functions, so these methods is not suitable for EMG analysis. To explore the signal distribution differences between different gestures, this paper uses EMD to decompose EMG signal into a series of IMFs according to the properties of EMG. And time-domain and frequency-domain features will be extracted from both raw EMG signal and decomposed IMFs. The different scale of features can be extracted by using EMD [29].

EMD is proposed by Huang et al. [30] in 1998, which is a new digital signal processing tool and is especially suitable for the analysis of non-linear and non-stationary biological electricity signal. EMD does not need any basic atom and decomposes signal by the time scale characters of the data, which is different from Fourier transform that is based on priori harmonic basis function and wavelet transform that is based on priori wavelet basis function. Instead, a decomposition procedure, known as the sifting process, is employed in EMD. The overall procedure is data-driven and adaptive and makes no assumptions about the input time series. The aim of EMD is to decompose raw signal into a series of IMFs. Huang N E et al. think all signals are consisted of a number of IMFs and combined signal will form if IMFs overlap together. An IMF represents a simple oscillatory function satisfying two conditions: firstly, the number of zero crossings and the number of local extrema are either equal or differ by one; secondly, the local average defined by the average of local maximum and local minimum envelops is equal to zero.

EMD is suitable for the analysis of EMG, as it can adaptively decompose original signal according to its time scale characters. On condition of raw EMG $EMG(t)$ is given, the procession of EMD is described in Algorithm 1.

After EMD, raw EMG signal $EMG(t)$ is decomposed into the sum of n IMFs $imf_i(t), i = 1, 2, \ldots, n$ and one residual error $x_n(t)$: $x_0(t) = \sum_{i=1}^{n} imf_i(t) + x_n(t)$, where $imf_i(t)$ expresses the fine-grained properties of original signal because it contains the local character of raw $EMG(t)$ at different scales. Thus, we will extract features from raw EMG signal $EMG(t)$ and n IMFs $imf_i(t), i = 1, 2, \ldots, n$ in time domain and frequency domain respectively in this paper. The extracted fine-grained features can express the distribution differences of EMG and can be used to recognize hand gesture precisely.

Algorithm 1 Empirical mode decomposition.

Input: $EMG(t)$

Output: $imf_1(t), imf_2(t), \ldots, imf_n(t), x_n(t)$

1: initialize $x_0(t) = EMG(t), i = 1$;
2: initialize $h_0(t) = x_{i-1}(t), j = 1$;
3: get local extreme point $h_{j-1}(t)$;
4: use local maxima and local minima of $h_{j-1}(t)$ to form upper envelope $e_{max}(t)$ and lower envelope $e_{min}(t)$ with Cubic Spline Interpolation;
5: calculate the mean $m_{j-1}(t) = \frac{e_{max}(t)+e_{min}(t)}{2}$;
6: $h_j = h_{j-1}(t) - m_{j-1}(t)$
7: if $h_j(t)$ is IMF, then $imf_i(t) = h_j(t)$; otherwise, $j = j + 1$, turn to 3;
8: $x_i(t) = x_{i-1} - imf_i(t)$;
9: if the number of extreme points of $x_i(t)$ is more than two, the $i = i + 1$, turn to 2; otherwise, decomposition ends, $x_i(t)$ is residual error, the result of this algorithm is $x_0(t) = \sum_{i=1}^{n} imf_i(t) + x_n(t)$.

3.2 Sequential features-based wearing position prediction method

The distribution of EMG signal sensed in different positions differs greatly due to the position-dependent property of EMG. Thus, the recognition model built by EMG sensed in specific position is hard to be used to distinguish hand gesture in other positions. So the wearing position prediction of EMG armband is essential to realize high-accuracy hand gesture recognition system. Usually, the position change happens in two conditions. One is when the armband wears just and users may put it on forearm with rotation of any angles. Another is happened during the using process. With the influence of outside force, position shift will occur inevitably. From the analysis above, we can know that the position change of EMG armband happens infrequently. So the position of EMG armband is not only relevant to current EMG but also has strongly temporal locality. To be more specific, the current position of EMG armband is relevant to the previous moments' signal. This paper proposes a sequence wearing position prediction method according to the temporal locality of EMG sensor's position.

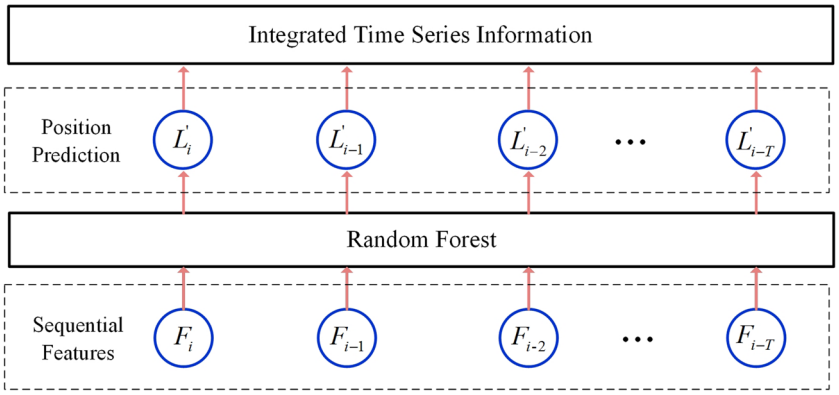

Fig. 2 Sequential features-based wearing position prediction method

Specifically, the position of EMG armband changes little in continuous time window $W_{i-T}, W_{i-T+1}, \ldots, W_{i-1}, W_i$, So $L_{i-T}, L_{i-T+1}, \ldots, L_{i-1}, L_i$ has strongly temporal locality. The position prediction method predicts EMG sensor's wearing position L_i by signal's distributions of current EMG signal and previous T moments' EMG signal.

Temporal sequential features-based method realizes the position prediction of hand gesture by Random Forest (RF), and the framework of this method is showed in Fig. 2. $F_i, F_{i-1}, F_{i-2}, \ldots, F_{i-T}$ are the features of current and previous T moments' EMG. $L'_i, L'_{i-1}, L'_{i-2}, \ldots, L'_{i-T}$ are corresponding position prediction results. So the final position prediction result of current moment is

$$L_i = \frac{\sum_{j=0}^{T} k_j \times L'_{i-j}}{\sum_{=0}^{T} k_j} \tag{1}$$

where, k_j is the weight of moment $i - j$, L_i is the final position prediction result fused the features of current and previous T moments'. The proposed position prediction method takes advantages of the temporal locality of wearing position, increasing the accuracy and stability of position prediction by exploring the correlation between current position and previous position. Lately, this paper will construct hand gesture recognition model using result of position prediction and current EMG in order to solve the accuracy decline problem caused by the change of wearing position.

3.3 Wearing position-based hand gesture recognition method

3.3.1 Hand gesture expression in Standard Space

In the overall process, the expression of EMG signal is a basic and key problem. In order to realize consistent representation, a natural and intuitive idea is to fix the position of the wearable device. However, in real application scenario, the requirement to fix position is not only disadvantage to achieve natural and harmonious gesture recognition, but also cannot be satisfied when the position shift occurs with the influence of outside force. So, we define Standard Space, where the distribution of EMG is insensitive to wearing position. According to wearing position prediction result, we represent original signal in this space to achieve consistent expression of cross-position gesture.

Standard Space is defined on the hypothesis that the electrodes of armband is distributed evenly, which is a regular status of this equipment. Assuming that there is a group of EMG collecting points $Q_1, Q2, \ldots, Q_w, w = E_{num}$ on the upper of forearm, where E_{num} is the number of electrodes. And there is a standard collecting point P on EMG armband. The standard wearing position is the condition that the collecting point P and Q_1 coincide, satisfied the requirement that $\angle P O Q_1 = 0$ as showed in Fig. 3a. The expression of EMG signal in this condition is Standard Space representation. In addition, we also define

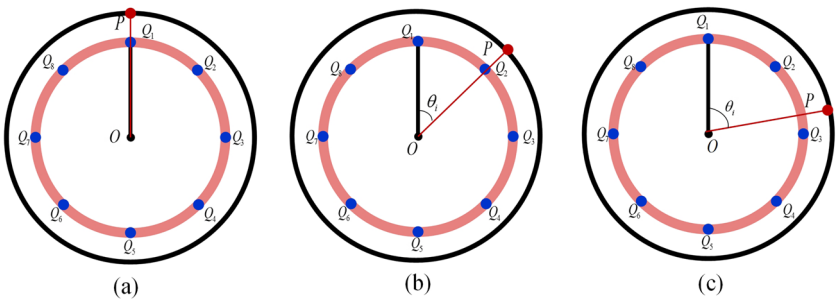

Fig. 3 **a** Standard Space expression, supposing $E_{num} = 8$. **b** Grid rotation, the angle of rotation $\theta_i = 2\pi \cdot k/E_{num}, k \in \{0, 1, \ldots, E_{num} - 1\}$. **c** Non-grid rotation, satisfied $\theta_i = 2\pi \cdot k/E_{num}, k \in [0, E_{num}) \wedge k \notin \{0, 1, \ldots, E_{num} - 1\}$

two wearing patterns, grid rotation and non-grid rotation, according to the angle of rotation. The grid rotation and non-gird rotation are showed in Fig. 3b, c respectively.

When the wearing position L_i of EMG armband is known, the mapping relation between L_i and $\angle POQ_1 = 0$ is $\angle POQ_1 = 2\pi \cdot (L_i - 1)/E_{num}$. If L_i is an integer, the wearing pattern is grid rotation and the rotation angle is $\theta_i = 2\pi \cdot k/E_{num}, k \in \{0, 1, \ldots, E_{num} - 1\}$; If L_i isn't an integer, the wearing pattern is non-grid rotation and the rotation angle is $\theta_i = 2\pi \cdot k/E_{num}, k \in [0, E_{num}) \wedge k \notin \{0, 1, \ldots, E_{num} - 1\}$. The strategy of Standard Space representation can be listed as follows in both grid rotation and non-grid rotation conditions:

Grid rotation, $\theta_i = 2\pi \cdot k/E_{num}, k \in \{0, 1, \ldots, E_{num} - 1\}$. This is a special rotation condition satisfied the requirement that $k = L_i - 1$, and the transformation strategies of EMG sensor's position and EMG signal are

$$Q_j \leftarrow Q_{v(j+L_i-1)}, j = 1, 2, \ldots, E_{num} \tag{2}$$

$$EMG'_{i,j} = EMG_{i,v(j+L_i-1)}, j = 1, 2, \ldots, E_{num} \tag{3}$$

where

$$v(i) = \frac{i-1}{E_{num}} + 1 \tag{4}$$

Supposing $E_{num} = 8, r = 5$, the mapping relation is listed in Table 1. As Table 1 shows, wearing positions Q_5, Q_6, Q_7, Q_8, Q_1, Q_2, Q_3, Q_4 are mapped to Q_1, Q_2, Q_3, Q_4, Q_5, Q_6, Q_7, Q_8, respectively. Features EMG_5, EMG_6, EMG_7, EMG_8, EMG_1, EMG_2, EMG_3, EMG_4 are mapped to EMG'_1, EMG'_2, EMG'_3, EMG'_4, EMG'_5, EMG'_6, EMG'_7, EMG'_8, respectively.

Non-grid rotation, $\theta_i = \frac{2\pi \cdot k}{E_{num}}, k \in [0, E_{num}) \wedge k \notin \{0, 1, \ldots, E_{num} - 1\}$, where $k = L_i - 1$. The approximate value of L_i is calculated firstly: $L'_i = \lfloor L_i + \frac{1}{2} \rfloor$, and the transformation strategy of EMG sensor's position and EMG signal are

$$Q_j \leftarrow \begin{cases} w_1 \cdot Q_{v(j+L'_i)} + w_2 \cdot Q_{v(j+L'_i-1)} & L'_i > L_i \\ w_2 \cdot Q_{v(j+L'_i)} + w_1 \cdot Q_{v(j+L'_i-1)} & L'_i < L_i \end{cases} \tag{5}$$

$$EMG_{i,j} \leftarrow \begin{cases} w_1 \cdot Q_{i,v(j+L'_i)} + w_2 \cdot Q_{i,v(j+L'_i-1)} & L'_i > L_i \\ w_2 \cdot Q_{i,v(j+L'_i)} + w_1 \cdot Q_{i,v(j+L'_i-1)} & L'_i < L_i \end{cases} \tag{6}$$

where

$j = 1, 2, \ldots, E_{num}$

$w_1 = |L'_i - L_i|$

$w_2 = 1 - w_1$

Table 1 The hand gesture expression in Standard Space

Position	Feature
$Q_5 \rightarrow Q_1$	$EMG'_{i,1} = EMG_{i,5}$
$Q_6 \rightarrow Q_2$	$EMG'_{i,2} = EMG_{i,6}$
$Q_7 \rightarrow Q_3$	$EMG'_{i,3} = EMG_{i,7}$
$Q_8 \rightarrow Q_4$	$EMG'_{i,4} = EMG_{i,8}$
$Q_1 \rightarrow Q_5$	$EMG'_{i,5} = EMG_{i,1}$
$Q_2 \rightarrow Q_6$	$EMG'_{i,6} = EMG_{i,2}$
$Q_3 \rightarrow Q_7$	$EMG'_{i,7} = EMG_{i,3}$
$Q_4 \rightarrow Q_8$	$EMG'_{i,8} = EMG_{i,4}$

3.3.2 Random Forest-based hand gesture recognition

RF [31] is a kind of resemble machine learning algorithm, which is known for its advantage of high classification accuracy, low generalization error, and low algorithm strength. RF has showed excellent performance in many fields. The EMG signal used in this paper consists of multi-channels and every channel is decomposed into a series of fine-grained components. Therefore, we takes advantages of RF's lightweight and no feature selection requirement to realize gesture recognition in this scenario.

The RF used in this paper is composed of N CART [32], and the depth of every CART is D. The optimal feature selection strategy of CART is Gini Index, and the optimal two-valued segmentation point is also determined by Gini Index. The decision process using Gini Index is the process of finding the best classification feature and segmentation point that can increase Gini Index maximally:

$$\arg\max_{f,\alpha}(Gini - GiniLeft - GiniRight) \tag{7}$$

$$Gini = 1 - \sum_{k=1}^{G} p_k \times p_k \tag{8}$$

where $Gini$, $GiniLeft$, $GiniRight$ stand for the Gini Index of parent node, left child node, and right child node, respectively. f is the classification feature and α is the decision threshold. p_k is the probability of the k^{th} hand gesture in current feature space. G is the total number of gestures. For a fixed hand gesture set, Gini Index expresses the uncertainty of this hand gesture set. And if this gesture set is more uncertain, the Gini Index is larger.

The framework of RF-based hand gesture recognition method is showed in Fig. 4. In the process of constructing RF, we assume the training set is S and the feature set

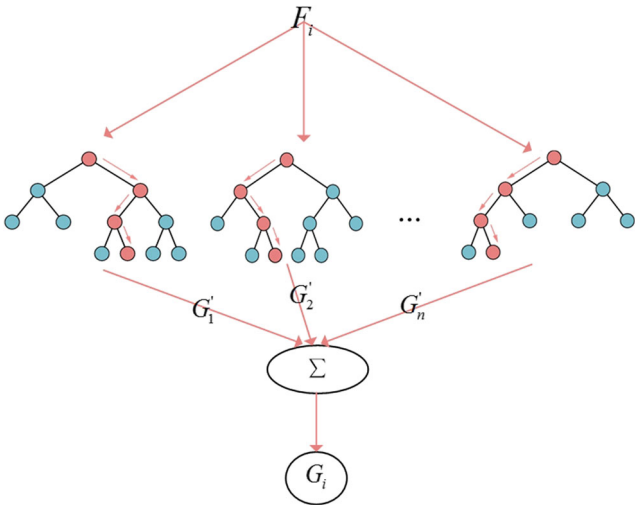

Fig. 4 Hand gesture recognition based on Random Forest

is C. For every CART, the training set $S(i)$ is selected from set S by replacement sampling, and the size of $S(i)$ is equal to S. In the training process of every CART, the feature subset C' is selected from feature set C by sampling without replacement on condition that current node is not satisfied terminable requirement. The constructed feature set contains $|C'|$ kinds of features. And the optimal feature will be selected from the subset C'. The decision process is based on feature F_i in Standard Space. If the n^{th} CART's prediction result is $P_{i,j,n}$, the final classification result merged N CARTs is

$$G_i = \arg\max_j \{\sum_{n=1}^{N} P_{i,j,n} | j = 1, 2, \ldots, G\} \quad (9)$$

4 Experimental analysis

4.1 Experimental setting

In order to verify the effectiveness and robustness of the proposed method, we design a hand gesture set [9], which includes finger movement, wrist movement, and other kinds of movement. The detail of each hand gesture is showed in Fig. 5.

We use the wearable myoelectric armband Myo from Thalmic Labs as our experimental instrument. Myo has eight electrical chips, which are evenly distributed on the surface. Myo can be attached to user's upper forearm with the rotation of any angle and its sampling rate is 200 Hz. Before the experiments, we mark the evenly distributed EMG collection points on subject's forearm as $Q_1, Q_2, Q_3, Q_4, Q_5, Q_6, Q_7, Q_8$, as showed in Fig. 6. In addition, we mark the benchmark signal point on Myo as P, which is showed in Fig. 7.

As the non-grid rotation can be approximated to grid rotation, we only explore this special condition in our experiment. Myo is attached on subject's forearm and rotated by an angle of $(2k-1)\cdot\pi/8, k = 0, 1, \ldots, 7$ respectively and for each rotation angle, the data collection process repeats ten times. In every repeat, subject is required to make the 15 predefined hand gestures orderly. At the interval of each gesture data collection, subject has a 5-s break and the collection time of every gesture lasts 20 s. To regularize the movement of subject, the standard gestures are showed before the beginning. And we also record the movement of subject by camera to make sure that the gesture can be segmented correctly and the movement of subject is performed standardly. Finaly, about 27,000 hand gestures are collected.

4.2 Preprocessing and feature extraction

As all gestures used are static gesture, we utilize sliding window to segment the gesture. The length of each window is 1 s and its overlay is 50%, which means the minimum interval is 0.5 s. After segmentation, we use EMD to resolve complicated EMG into a series of IMFs, which can express the component of the EMG in different scales. Figure 8 depicts one of the eight channels of EMG along with the corresponding first five IMFs of "Thumb" gesture. The first line of Fig. 8 is the raw signal, lines 2–6 are the five IMFs, and line 7 is the residual error. From Fig. 8, we can know

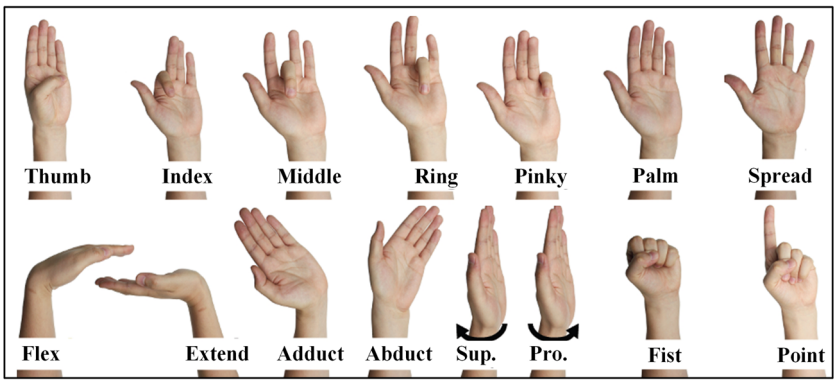

Fig. 5 The detail of each hand gesture

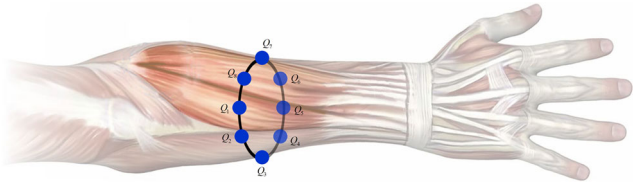

Fig. 6 Signal collection points on upper forearm

that raw signal and its IMFs express the distribution of EMG in different scales and more fine-grained information of gesture can be showed by the combination of these components above.

Generally, most of the attempts to extract features from EMG signal can be classified into three categories, including time domain, frequency domain, and time-frequency domain [33]. We considered only former two categories because they are computing efficient and they have been used in research widely [34]. In feature extraction process, we separately extracted seven time-domain features and three frequency-domain features from raw EMG and IMF signal, which are described as Table 2 [35], where x_i represents the raw sEMG signal and N is the length of x_i. PSD_i means the power spectrum density and M means the length of PSD_i. A_i and f_i indicate the magnitude spectrum and frequency, respectively.

4.3 Wearing position prediction

Wearing position of armband is predicted by sequential features-based method. In the experimental process, current and previous $T = 4$ moments' EMG signal are used to predict current wearing position. And the parameter of RF is that the scale of RF is $N = 100$ and the depth of every CART is $D = 8$. Using tenfold cross validation, the position prediction result is showed in Fig. 9 and Table 3. As showed in Fig. 9 and Table 3, the final prediction accuracy is 94.74% with our proposed sequential features-based method. Compared with the methods without EMD and sequential features, the accuracy promotes 7.09% from 87.65%. Compared with the methods without sequential features, the accuracy promotes 0.80% from 93.94%.

Fig. 7 Benchmark signal point on Myo

4.4 Standard Space expression and hand gesture recognition

Original EMG can be represented in Standard Space according to the position prediction result L_i. Figure 10 depicts the eight channels of raw EMG along with the corresponding Standard Space expression for the "Spread" gesture and "Fist" gesture. The first two rows are the signal distribution of "Spread" gesture, where the first row is the raw signal and the second row is the signal in Standard Space. The last two rows are the signal distribution of "Fist" gesture, where the third row is the raw signal and the second row are the signal in Standard Space. The different columns stand for armband's different wearing positions $Q_1, Q_2, \ldots, Q_8$, where the i^{th} column is the corresponding information in position Q_i. In every line chart, the different color stands for the signal of different electrodes. Comparing the arrangement of color in the first two rows or the last two rows, it is obvious that the color order in the upper chart is messy across different columns, which stands for the randomness of original signal across different wearing positions. While the color distribution in the lower chart is order, which stands for the regularity of signal in Standard Space across different wearing positions. Comparing the distribution of the original signal and signal in Standard Space at the same wearing position, it is obvious that the signal in Standard Space can avoid the distribution shift caused by wearing position and increase the accuracy and stability of gesture recognition.

Hand gesture recognition model is constructed by RF, which is composed of $N = 100$ CARTs and the depth of every CART is $D = 8$. The recognition accuracy of eight wearing positions $Q_1, Q_2, \ldots, Q_8$ and the average recognition accuracy are showed in Fig. 11 and Table 4. To show the effectiveness of the proposed method, there are three comparison experiments, which are the method without EMD and Standard Space representation of signal, the method without Standard Space representation of signal, and our proposed RF-based hand gesture recognition method. As we can know from Fig. 11, the average classification accuracy using the proposed method is 91.47% for eight wearing positions. Compared with the method using RF solely, the upgrading of accuracy is 10.12% and the upgrading of accuracy is 5.13% compared with adding EMD method. According to experimental result, compared with the method without EMD and Standard Space representation of signal, the proposed

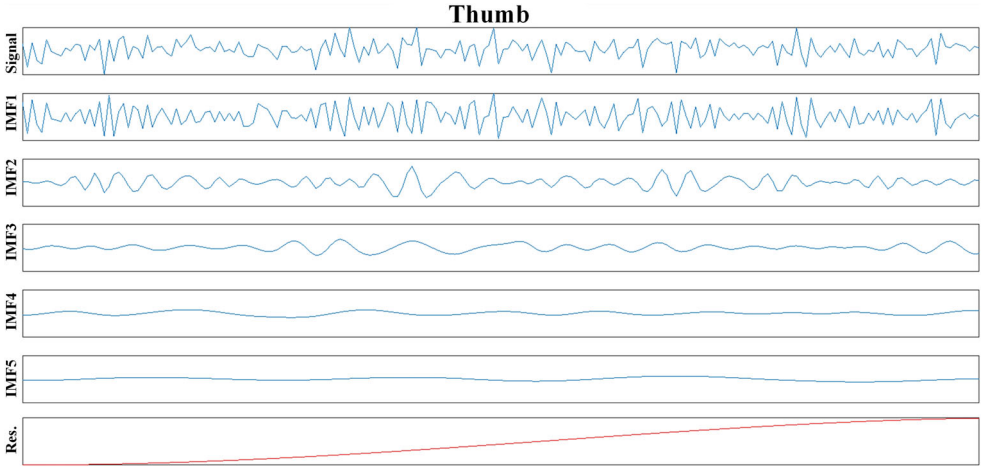

Fig. 8 The raw EMG of "Thumb" gesture and corresponding IMF

Table 2 Feature extraction

Extracted feature	Description
Mean absolute value	$MAV_k = \frac{1}{N}\sum_{i=1}^{N} \lvert x_i \rvert$
Modified mean absolute value 1	$MMAV1_k = \frac{1}{N}\sum_{i=1}^{N} w_i \lvert x_i \rvert \; w(i) = \begin{cases} 1, & 0.25N \le i \le 0.75N \\ 0.5, & otherwise \end{cases}$
Modified mean absolute value 2	$MMAV2_k = \frac{1}{N}\sum_{i=1}^{N} w_i \lvert x_i \rvert \; w(i) = \begin{cases} 1, & 0.25N \le i \le 0.75N \\ \frac{4i}{N}, & 0.25N > i \\ \frac{4(i-N)}{N}, & 0.75N < i \end{cases}$
Mean absolute value slope	$MAVS_k = MAV_{k+1} - MAV_K$
Root mean square	$RMS_k = \sqrt{\frac{1}{N}\sum_{i=1}^{N} x_i^2}$
Variance	$VAR_k = \frac{1}{N}\sum_{i=1}^{N} x_i - \hat{x}^2$
Waveform length	$WL_k = \sum_{i=1}^{N-1} x_{i+1} - x_i$
Frequency median	$F_{MD} = \frac{1}{2}\sum_{i=1}^{M} PSD_i$
Frequency mean	$F_{MN} = \frac{\sum_{i=1}^{M} f_i PSD_i}{\sum_{i=1}^{M} PSD_i}$
Modified frequency mean	$MF_{MN} = \frac{\sum_{j=1}^{M} f_j A_j}{\sum_{j=1}^{M} A_j}$

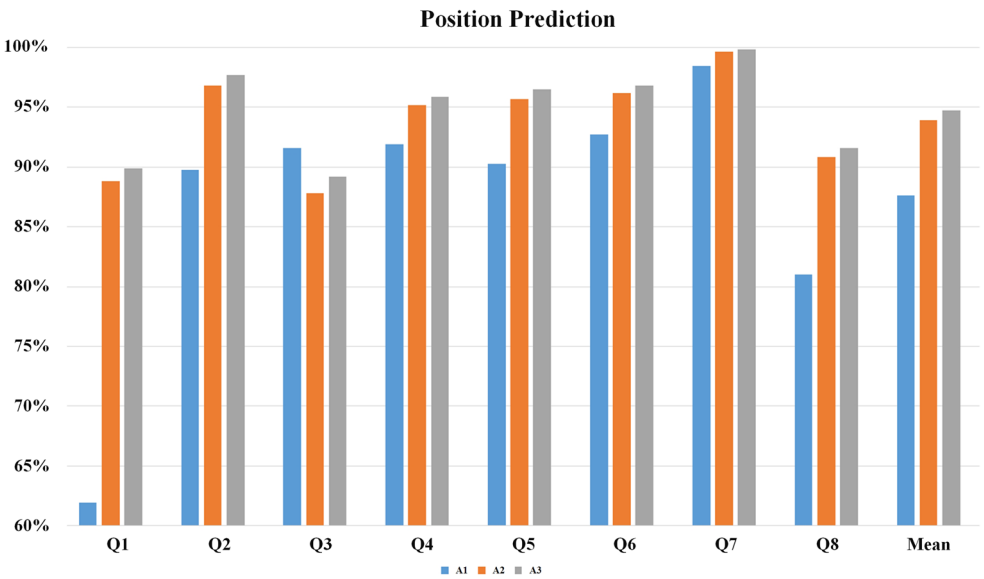

Fig. 9 The result of wearing position prediction

Table 3 The result of wearing position prediction

	A_1	A_2	A_3	C_{1-3}	C_{2-3}
$Q1$	61.95	88.84	89.92	27.97	1.08
$Q2$	89.79	96.79	97.67	7.87	0.88
$Q3$	91.62	87.84	89.22	− 2.40	1.38
$Q4$	91.89	95.19	95.84	3.96	0.66
$Q5$	90.30	95.70	96.48	6.18	0.78
$Q6$	92.73	96.17	96.83	4.10	0.66
$Q7$	98.48	99.63	99.83	1.34	0.20
$Q8$	80.99	90.83	91.62	10.63	0.79
Mean	87.65	93.94	94.74	7.09	0.80

A_1 stands for the method without EMD and sequential features; A_2 stands for the method without sequential features; A_3 stands for the proposed sequential features-based method; C_{1-3} stands for accuracy promoting compared A_3 with A_1; and C_{2-3} stands for accuracy promoting compared A_3 with A_2. Unit: %

method acquires maximally accuracy lifting at Q_3 position and the lifting is 21.61%, but the accuracy lifts minimally at Q_5 position and the lifting is 4.72%.

Coincidentally, if using the method without EMD and Standard Space representation of signal, the classification accuracy is 66.35% at Q_3 position and it is the lowest among eight positions; the classification accuracy is 89.15% at Q_5 position and it is the highest among eight positions. Possible explanation is that Q_3 depends on wearing position strongly, so the accuracy is the lowest using traditional method, and the accuracy lifts greatly using the method in this paper. In contract, Q_5 depends on wearing position weakly, so the accuracy lifts little on the condition that the original classification accuracy is high enough. The analysis above shows that our method can not only increase classification accuracy, but also upgrade classification stability. The analysis of standard deviation in Fig. 12 verifies the guess above. As shown in Fig. 12, the standard deviation using the proposed method is 0.0212. Compared with the method without EMD and Standard Space representation of signal, the standard deviation reduces 0.0511 and compared with the method without Standard Space representation of signal, the standard deviation reduces 0.0427.

The confusion matrix using proposed method is showed in Fig. 13, where the column is the actual gesture and the row is the predicted gesture. The comparison of accuracy of three methods and the accuracy lifting are showed in Table 5. As we can know from the analysis of Fig. 13 and Table 5, there is accuracy lifting using the proposed method for all hand gestures, where the accuracy lifting is the lowest for Palm gesture and the lifting is 2%; the accuracy lifting is the highest for Index gesture and the lifting is 16%. Possible explanation is that Index gesture depends on wearing position strongly, so the accuracy lifts greatly using the proposed method. In contract, Palm gesture depends on wearing position weakly, so the accuracy lifts little. From the analysis aforementioned, we can know that

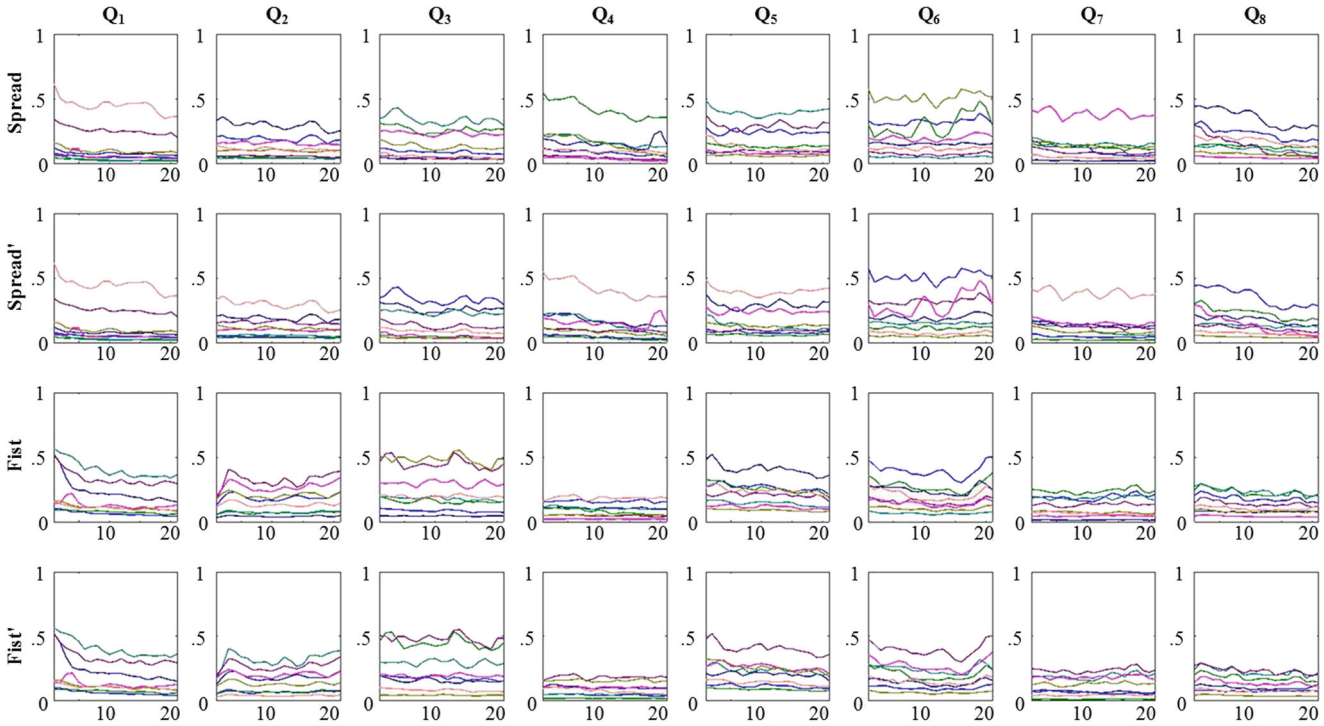

Fig. 10 The distribution of EMG

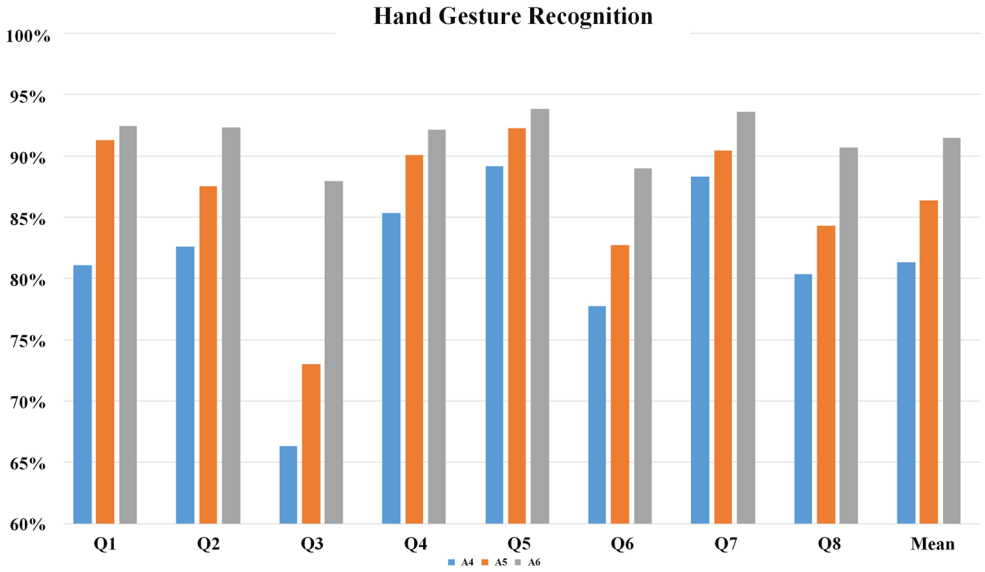

Fig. 11 The result of hand gesture classification

Table 4 The result of hand gesture classification

	A_4	A_5	A_6	C_{4-6}	C_{5-6}
$Q1$	81.09	91.28	92.44	1.16	11.35
$Q2$	82.60	87.54	92.30	4.76	9.70
$Q3$	66.35	73.04	87.96	14.92	21.61
$Q4$	85.36	90.07	92.16	2.09	6.80
$Q5$	89.15	92.26	93.87	1.61	4.72
$Q6$	77.78	82.71	88.97	6.26	11.20
$Q7$	88.32	90.44	93.57	3.13	5.26
$Q8$	80.37	84.28	90.68	6.40	10.31
Mean	81.35	86.34	91.47	5.13	10.12

A_4 stands for the method without EMD and Standard Space representation of signal; A_5 stands for the method without Standard Space representation of signal; A_6 stands for our proposed RF-based hand gesture recognition method; C_{4-6} stands for accuracy increasing compared A6 with A4; and C_{5-6} stands for accuracy increasing compared A6 with A5. Unit: %

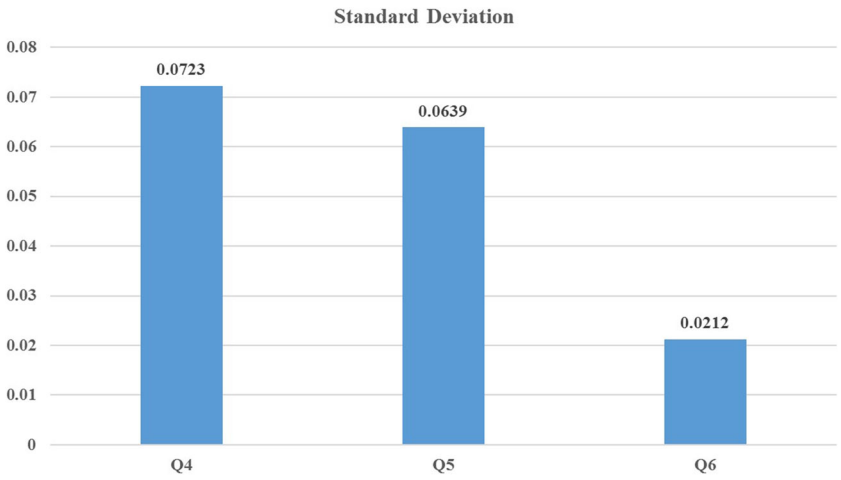

Fig. 12 The result of standard deviation for all positions

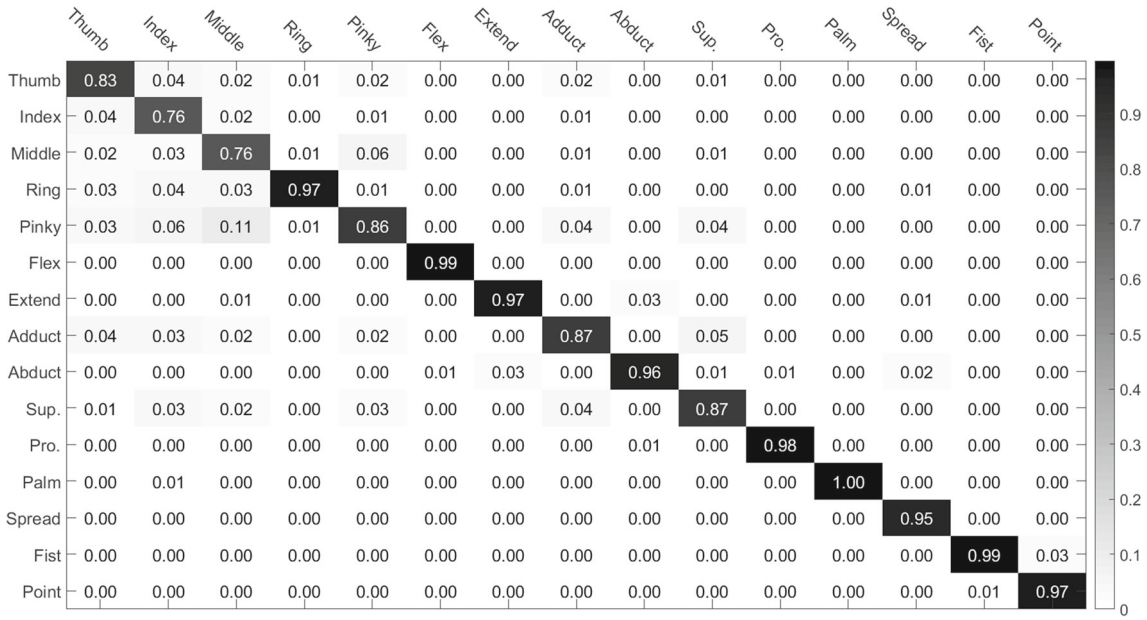

Fig. 13 The confuse matrix for hand gesture classification

the proposed method can not only increase classification accuracy, but also upgrade classification stability among different hand motions. The analysis of standard deviation in Fig. 14 verifies our guess. As shown in Fig. 14, the standard deviation for the fifth gestures Pinky using our method is 0.0839. Compared with the method without EMD and representation of signal, the standard deviation reduces 0.0299 and compared with the method without representation of signal, the standard deviation reduces 0.034.

Table 5 The classification accuracy for all gestures

	A_1	A_2	A_3	C_{1-3}	C_{2-3}
Thumb	69	75	83	14	8
Index	60	59	76	16	17
Middle	70	75	76	6	1
Ring	83	93	97	14	4
Pinky	72	80	86	14	6
Flex	95	96	99	4	3
Extend	84	97	97	13	0
Adduct	72	80	87	15	7
Abduct	83	91	96	13	5
Sup.	72	73	87	15	14
Pro.	86	95	98	12	3
Palm	98	99	100	2	1
Spread	89	94	95	6	1
Fist	95	98	99	4	1
Point	90	91	97	7	6

A_4 stands for the method without EMD and Standard Space representation of signal; A_5 stands for the method without Standard Space representation of signal; A_6 stands for our proposed RF-based hand gesture recognition method; C_{4-6} stands for accuracy increasing compared A6 with A4; and C_{5-6} stands for accuracy increasing compared A6 with A5. Unit: %

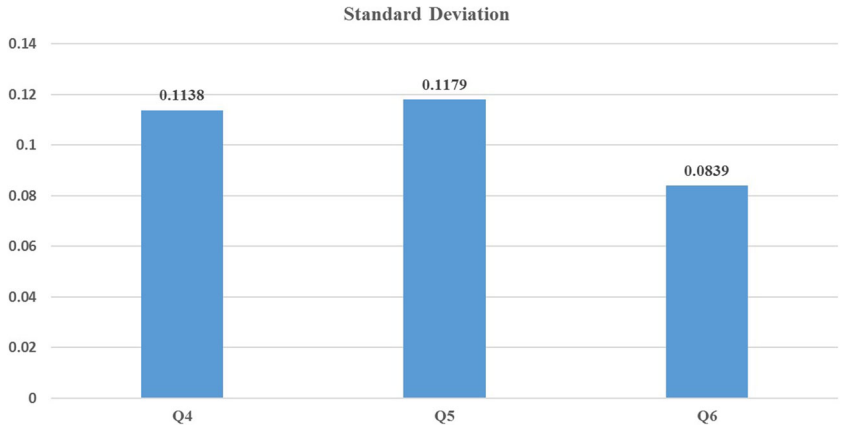

Fig. 14 The result of standard deviation for all gestures

5 Conclusion and future work

This paper proposes a wearing-independent hand gesture recognition method based on EMG acquired by EMG armband. EMG armband which usually contains electrodes that is mounted around the user's forearm is a kind of more ergonomic wearable EMG devices. Compared with traditional equipment whose electrodes are either precisely attached on muscle or array-like arrangement that can capture the activity under a certain area of the upper forearm, armband can get a better user experience. At the preprocess period, EMD is applied to decompose raw data into a series of IMFs. And seven time-domain features and three frequency-domain features are extracted from original signal and decomposed IMFs. According to the temporal localities of wearing position of armband, sequential features-based method is used to predict the placement of device. The result helps unify the features to the proposed Standard Space, where the expression of EMG is position independent. Then, with the unified signals, fine hand gesture can be recognized accurately and robustly by RF. The innovations of this paper can be listed as follows: (1) Using EMD to extract the fine-grained EMG signal's features. EMG is characterized by non-linearity and non-stationary and fine-grained feature extraction strategy can upgrade the accuracy of position prediction and hand gesture recognition. (2) Putting forward sequential features based position prediction method. The wearing position of EMG armband shows temporal localities, so we predict the current wearing position using current and previous EMG data. (3) Representing EMG in Standard Space. The raw EMG is unified to Standard Space according to the result of wearing position prediction, and the classification accuracy and stability lifted our proposed method.

However, there are some limits of our method. Now, the proposed algorithm can recognize hand gesture accurately on condition of grid rotation, but the prediction for non-grid rotation is approximated to the former case. It is obvious this assumption will reduce the recognition accuracy in some degree. So, we will focus on condition of non-grid rotation in future work. In addition, the main purpose of this paper is to explore the influence of wearing position. So we only use static gestures, the influence of wearing position to dynamic gestures is the future work.

Funding information This work is supported in part by the National Key Research and Development Plan of China (No. 2017YFB1002801), Natural Science Foundation of China (No.61502456, No.61572471), Beijing Science and Technology Committee, and Brain Science Research Program of Beijing (No.Z161100000216140).

References

1. Ahsan MR, Ibrahimy MI, Khalifa OO (2009) EMG signal classification for human computer interaction: a review. Eur J Sci Res 33(3):480–501
2. Song J, Sörös G, Pece F et al (2015) Real-time hand gesture recognition on unmodified wearable devices. In: IEEE Conference on computer vision and pattern recognition
3. Ducloux J, Colla P, Petrashin P et al (2014) Accelerometer-based hand gesture recognition system for interaction in digital TV. In: 2014 IEEE International on instrumentation and measurement technology conference (I2MTC) proceedings. IEEE, pp 1537–1542
4. Nandakumar R, Iyer V, Tan D et al (2016) FingerIO: using active sonar for fine-grained finger tracking. In: Proceedings of the 2016 CHI conference on human factors in computing systems. ACM, pp 1515–1525
5. Lien J, Gillian N, Karagozler ME et al (2016) Soli: ubiquitous gesture sensing with millimeter wave radar. ACM Trans Graph (TOG) 35(4):142
6. McIntosh J, Marzo A, Fraser M et al (2017) EchoFlex: hand gesture recognition using ultrasound imaging. In: Proceedings of the 2017 CHI conference on human factors in computing systems. ACM, pp 1923–1934
7. Zhang X, Chen X, Li Y et al (2011) A framework for hand gesture recognition based on accelerometer and EMG sensors. IEEE Trans Syst Man Cybern-Part A: Syst Humans 41(6):1064–1076
8. Zhang X, Chen X, Wang W et al (2009) Hand gesture recognition and virtual game control based on 3D accelerometer and EMG sensors. In: Proceedings of the 14th international conference on intelligent user interfaces. ACM, pp 401–406

9. McIntosh J, McNeill C, Fraser M et al (2016) EMPress: practical hand gesture classification with wrist-mounted EMG and pressure sensing. In: Proceedings of the 2016 CHI conference on human factors in computing systems. ACM, pp 2332–2342
10. Benatti S, Casamassima F, Milosevic B et al (2015) A versatile embedded platform for EMG acquisition and gesture recognition. IEEE Trans Biomed Circ Syst 9(5):620–630
11. Myo arm band [Online]. Available: http://www.myo.com/
12. gForce arm band [Online]. Available: http://www.oymotion.com/
13. DTing arm band [Online]. Available: http://www.dtingsmart.com/
14. DTing arm band [Online]. Available: http://econtek.cn/
15. Mesa I, Rubio A, Tubia I et al (2014) Channel and feature selection for a surface electromyographic pattern recognition task. Expert Syst Appl 41(11):5190–5200
16. Castellini C, Fiorilla AE, Sandini G (2009) Multi-subject/daily-life activity EMG-based control of mechanical hands. J Neuroengi Rehab 6(1):41
17. Kim J, Mastnik S, André E (2008) EMG-based hand gesture recognition for realtime biosignal interfacing. In: Proceedings of the 13th international conference on intelligent user interfaces. ACM, pp 30–39
18. Assad C, Wolf M, Theodoridis T et al (2013) Biosleeve: a natural EMG-based interface for HRI. In: Proceedings of the 8th ACM/IEEE international conference on human-robot interaction. IEEE Press, pp 69–70
19. Samadani AA, Kulic D (2014) Hand gesture recognition based on surface electromyography. In: 2014 36th Annual International conference of the IEEE engineering in medicine and biology society (EMBC). IEEE, pp 4196–4199
20. Amma C, Krings T, Böer J et al (2015) Advancing muscle-computer interfaces with high-density electromyography. In: Proceedings of the 33rd Annual ACM conference on human factors in computing systems. ACM, pp 929–938
21. Ellis MD, Acosta AM, Yao J et al (2007) Position-dependent torque coupling and associated muscle activation in the hemiparetic upper extremity. Exper Brain Res 176(4):594–602
22. Hargrove LJ, Englehart K, Hudgins B (2007) A comparison of surface and intramuscular myoelectric signal classification. IEEE Trans Biomed Eng 54(5):847–853
23. Liu H, Hu B, Moore P (2015) HCI model with learning mechanism for cooperative design in pervasive computing environment. J Internet Technol 16(2):201–210
24. Matsubara T, Morimoto J (2013) Bilinear modeling of EMG signals to extract user-independent features for multiuser myoelectric interface. IEEE Trans Biomed Eng 60(8):2205–2213
25. Saponas TS, Tan DS, Morris D et al (2009) Enabling always-available input with muscle-computer interfaces. In: Proceedings of the 22nd Annual ACM symposium on user interface software and technology. ACM,pp 167–176
26. David RL, Cristian CL, Humberto LC (2015) Design of an electromyographic mouse. In: 2015 20th Symposium on signal processing, images and computer vision (STSIVA). IEEE, pp 1–8
27. Khushaba RN (2014) Correlation analysis of electromyogram signals for multiuser myoelectric interfaces. IEEE Trans Neural Syst Rehabil Eng 22(4):745–755
28. Lu Z, Chen X, Li Q et al (2014) A hand gesture recognition framework and wearable gesture-based interaction prototype for mobile devices. IEEE Trans Human-Mach Syst 44(2):293–299
29. Sapsanis C, Georgoulas G, Tzes A et al (2013) Improving EMG based classification of basic hand movements using EMD. In: 2013 35th Annual International conference of the IEEE engineering in medicine and biology society (EMBC). IEEE, pp 5754–5757
30. Huang NE, Shen Z, Long SR et al (1971) The empirical mode decomposition and the Hilbert spectrum for nonlinear and non-stationary time series analysis. In: Proceedings of the royal society of London A: mathematical, physical and engineering sciences, vol 454. The Royal Society 1998, pp 903–995
31. Breiman L (2001) Random forests. Mach Learn 45(1):5–32
32. Breiman L, Friedman J, Stone CJ et al (1984) Classification and regression trees[M]. CRC press
33. Oskoei MA, Hu H (2007) Myoelectric control systems—a survey. Biomed Signal Process Control 2(4):275–294
34. Phinyomark A, Limsakul C, Phukpattaranont P (2009) A novel feature extraction for robust EMG pattern recognition. arXiv:0912.3973
35. Rechy-Ramirez EJ, Hu H (2011) Stages for developing control systems using EMG and EEG signals: a survey. School of Computer Science and Electronic Engineering. University of Essex, pp 1744–8050